acta medica

ORIGINAL ARTICLE

Investigation of the anticancer, antimigration and antiangiogenesis effects of an oxadiazole derivative in two- and three-dimensional cultured Ishikawa and Huvec cells; *in vitro* and *in silico* studies

Muhammet Volkan Bülbül[1,5]
ORCID: 0000-0003-1526-2065

Arif Mermer[2,3]
ORCID: 0000-0002-4789-7180

Fatih Kocabaş[4]
ORCID: 0000-0001-8096-6056

Mervenur Kalender[5]
ORCID: 0000-0002-0885-3417

Bircan Kolbaşı Erkan[5]
ORCID: 0000-0001-7933-4262

İlknur Keskin[5]
ORCID: 0000-0002-7059-1884

[1] Department of Histology and Embryology, Faculty of Medicine, Ağrı Ibrahim Cecen University, Ağrı, Türkiye.

[2] Deparment of Biotechnology, University of Health Sciences, İstanbul, Türkiye.

[3] Experimental Medicine Application and Research Center, Validebag Research Park, University of Health Sciences, İstanbul, Türkiye.

[4] Department of Genetics and Bioengineering, Faculty of Engineering, Yeditepe University, İstanbul, Türkiye.

[5] Department of Histology and Embryology, School of Medicine, Istanbul Medipol University, İstanbul, Türkiye.

Corresponding Author: İlknur Keskin
E-mail: ilknurkeskin@medipol.edu.tr

Received: 14 October 2023, Accepted: 22 December 2023, Published online: 29 March 2024

ABSTRACT

Introduction: There are various methods used in cases of metastatic endometrial cancer. However, the prognosis is generally poor. Therefore, new anticancer agents are expected to exhibit the potential to prevent metastasis, as well as their effects on the viability of cancer cells. In in vitro conditions, the Ishikawa cell line represents endometrial adenocarcinoma and the Huvec cell line represents human umbilical vein endothelial cells. Oxadiazole derivatives may be promising new agents for endometrial cancer treatments by exhibiting anticancer and antiangiogenic properties.

Objective: The aim of this study was to examine the anticancer, antimigration and antiangiogenic effects of 5-[(4-Phenylpiperazine-1-yl)methyl]-1,3,4-oxadiazol-2-thiol (FP-Oxa) on co-cultured Ishikawa and Huvec cells.

Materials and Methods: In silico molecular docking, ADME and toxicity analyzes were performed for FP-Oxa. The effect on the viability of two- and three-dimensional mono- and co-culture models created with HUVEC and Ishikawa cells was evaluated by MTT analysis and IC_{50} values were calculated. The effect on the migration of two-dimensional cultured cells was determined by wound healing assay. Changes in VEGF expression in three-dimensional co-culture models were evaluated by immunofluorescence staining.

Results: As a result of in silico analyses, it was determined that FP-Oxa was within the oral bioavailability limits, exhibited class 4 toxicity, and had inhibition potential by binding to VEGR2. While FP-Oxa clearly inhibited migration in two-dimensionally cultured Ishikawa cells, it did not show the same level of success in Huvec and co-cultured cells. It was effective in reducing VEGF expression in three-dimensional co-cultures.

Conclusion: FP-Oxa may have various therapeutic effects on endometrial adenocarcinoma cells. It will be important to conduct biological activity studies in three-dimensional models that mimic the tumor structure created with different types of cancer cells.

Keywords: Endometrial carcinoma, molecular docking, multicellular spheroids, anticancer, VEGF

INTRODUCTION

Endometrial cancer (EC) is one of the most frequently diagnosed gynecological tumors worldwide [1]. Women with deep myometrial invasion, high-risk histological types such as serous or clear cell, or in the third stage of the disease are at increased risk for recurrence and/or metastasis [2]. Paclitaxel plus carboplatin therapy is the standard first-line chemotherapy for advanced, recurrent, and metastatic endometrial carcinoma [3]. Until recently, only 2 different treatments were specifically approved for use in metastatic cases, making it necessary to continue studies on the development of new anticancer agents in the chemotherapeutic treatment of endometrial cancer [4].

The blood vessel network that develops in the tumor microenvironment not only mediates the nutrition and oxygen supply of cancer cells, but also enables them to come into contact with the lymphatic network, causing metastasis [5]. It is known that vascular endothelial growth factor (VEGF) directly affects endothelial cells and changes cell migration, division and gene expression profiles [6]. Previous studies have shown that VEGF types are associated with the progression of endometrial cancer levels at different stages [7]. It has also been concluded that drugs such as Lenvatinib [8], Nintedanib [9], Brivanib [10] have the potential to prevent tumor progression by inhibiting the VEGF-VEGFR cascade. Human umbilical vein endothelial cells (Huvec) express VEGF-A, -B, -C and VEGF receptors R1, R2, and R3 [11]. In our study, co-culture models were established with endometrial adenocarcinoma cells (Ishikawa) and human umbilical vein endothelial cells (Huvec) to mimic the effects of VEGF, which promotes the progression of endometrial cancer *in vivo*.

Traditional two-dimensional (2D) cell culture models cannot represent the tumor microenvironment because they do not have a three-dimensional cell network and extracellular matrix found in the tumor structure [12]. Studies have shown that gene expression in three-dimensional cultures (3D) is closer to clinical expression profiles than those seen in 2D cultures [13]. Furthermore, it is thought that the different responses of 2D cultured cells and *in vivo* tumor cells to radiotherapy and chemotherapy may be a direct result of variation in spatial organization and cell-cell contacts [14].

The 1,3,4-oxadiazole ring, which is a widely used pharmacophore, has attracted attention of many studies in recent years due to its metabolic profiles and ability to form hydrogen bonds with the receptor site. 1,3,4-oxadiazole are bioisosteres of amides and esters that, due to the azole group (-N=C-O) in the oxadiazole core, increase lipophilicity affecting the drug's ability to reach the target by transmembrane diffusion, and may contribute to important pharmacokinetic properties [15]. 1,3,4-oxadiazoles demonsrate various biological activities such as anti-inflammatory, hypoglycemic, antianxiety, antidepressant, antiproliferative, antifungal, antibacterial and antitubercular [16]. Among them, different mono and di-substituted 1,3,4-oxadiazole exhibit potent antitumor activities against different cancer cell cultures with selective target [17].

In this study, it was aimed to investigate the biological activities of the compound, an oxadiazole derivative previously synthesized by our group [18] and which DNA gyrase activity studies (10.12 ± 0.14 μM) were performed, in 2D and 3D cell culture models. Drug target determination (drugability), absorption, distribution, metabolism, and excretion (ADME), toxicity, and molecular docking analysis of the compound we named 5-[(4-Phenylpiperazine-1-yl)methyl]-1,3,4-oxadiazol-2-thiol (FP-Oxa) were examined. The effect of FP-Oxa on Huvec and Ishikawa has been demonstrated in co-cultures developed to mimic the tumor microenvironment. Additionally, the effects on VEGF expressions in 3D culture models and changes in migration of 2D cultured cells were also analyzed.

MATERIALS and METHODS

In silico druglikeness analysis

The pharmacokinetics (ADME) properties, druglikeness, medicinal chemistry, and toxicity calculations were done by online web tools. The used web servers are that SwissADME [19], ProTox-II [20], SwissTargetPrediction [21], Boiled-Egg Method [22].

Toxicity analysis

The web-based Pro Tox II (https://tox-new.charite.de/protox_II/) free software was used for toxicity assessment and was calculated by entering the smile notation of the compound.

Molecular docking studies, ligand preparation

SDF files of ligands were generated using DataWarrior. Briefly, SMILES codes are used to generate conformers with setting as following: Random, Low Energy Bias, Torsions based on crystallographic database, energy minimization based on MMFF94s+ Force field. SD file version 3 with 3D atom coordinates has been used. The SDF files of known and potent VEGFR2 inhibitors (IC_{50}s of 12 nM-40 nM) were also generated and used for comparison purposes (Table 1).

Docking parameters and protein preparation

Human VEGFR2 ligand-binding domain in complex with benzimidazole-urea inhibitor (PDB ID: 2OH4) has been used to for docking studies. Briefly, crystal structure of protein was downloaded in pdb format from https://www.rcsb.org. Receptor structures were checked for incorrect charges and missing atoms and were optimized by removing water molecules, ions, and small molecules. A grid box with 26°Ax28°Ax26°A around the ATP binding pocket has been generated using AutoDockTools 1.5.6. Automated docking of ligands was performed with PaDelADV with as we have done previously [23].

Cell culture

Huvec (Human umbilical vein endothelial cell line-ATCC/CRL-1730) cells were cultured in DMEM F12K (21127022, Gibco) medium containing 10% FBS (FB-1001/500, Biosera), 1% streptomycin / penicillin (XC-A4110/100, Biosera) and 0.2% EGF solution. Ishikawa (endometrial cancer cell line-MERCK/99040201-1VL) cells were cultured in MEM (LM-E1149/500, Biosera) medium containing 10% FBS, 1% streptomycin/penicillin, 1% non-essential amino acid (XC-E1154/100, Biosera). Both cell lines were incubated at 37°C in a humidified atmosphere with 5% CO_2.

2D mono-culture and co-culture of huvec and ishikawa cells, MTT cell viability assay

Huvec and Ishikawa cells were seeded $1x10^4$ cells per well in 96 well-plate for monoculture model. For co-culture model, $5x10^3$: $5x10^3$ Huvec and Ishikawa cells were seeded per well in 96 well-plate. It was left to grow in an incubator with 5% CO_2 at 37°C. Huvec and Ishikawa cells were seeded for two-dimensional co-culture applications. In each well of an 96-well chamber, the medium of both cell lines was mixed in a ratio of 1: 1. After the cells become confluent, the 96-well microculture plates were treated with various concentrations (4-3-2-1-0.5 µM in DMSO) of FP-Oxa. Cells treated with %0.1 TritonX-100 (Millipore, 108603) were used as the positive control group, and cells not treated with FP-Oxa formed the negative control group. After 24 hours of incubation, medium FP-Oxa mixtures were aspirated. The wells were

Table 1. SMILES and information of molecules used in the docking study

Name	SMILES	Information
Ki20227	CC(C1=NC=CS1)NC(=O)NC2=C(C=C(C=C2)OC3=C4C=C(C(=CC4=NC=C3)OC)OC)OC	Ki20227 is an orally active and highly selective inhibitor of vascular endothelial growth factor receptor-2 (KDR/VEGFR-2, IC_{50}: 12 nM)
SKLB1002	CC1=NN=C(S1)SC2=NC=NC3=CC(=C(C=C32)OC)OC	SKLB1002 is a potent and ATP-competitive VEGFR2 inhibitor with IC_{50} of 32 nM.
CS-2660 (JNJ-38158471)	CCNC(=O)NC1=C(C=C(C=C1)OC2=NC=NC(=C2/C=N/OC)N)Cl	CS-2660 (JNJ-38158471) is a well tolerated, orally available, highly selective VEGFR-2 inhibitor with IC_{50} of 40 nM while it has no significant activity (>1 microM) against VEGFR-1 and VEGFR-3.
Taxifolin (Dihydroquercetin)	C1=CC(=C(C=C1[C@@H]2[C@H](C(=O)C3=C(C=C(C=C3O2)O)O)O)O)O	Taxifolin, type I inhibitor for VEGFR-2 kinase, is a flavonoid in many plants such as Taxus chinensis, Siberian larch, Cedrus deodara and so on.
Nintedanib (BIBF 1120)	CN1CCN(CC1)CC(=O)N(C)C2=CC=C(C=C2)N=C(C3=CC=CC=C3)C4=C(NC5=C4C=CC(=C5)C(=O)OC)O	Nintedanib (BIBF 1120, Intedanib, Vargatef, Ofev) is a potent triple angiokinase inhibitor for VEGFR1/2/3 with IC_{50} of 34 nM/13 nM/13 nM in cell-free assays.
FP-Oxa	Sc3nnc(CN1CCN(CC1)c2ccccc2)o3	This molecule has been developed in this study.

washed with PBS so as not to damage the cells. 200 microliters of MTT (Vybrant® MTT Cell Proliferation Assay Kit) solution, diluted 1:20 in medium, was added to each well. MTT solutions were aspirated after 3 hours of incubation. Formazan salts were dissolved by adding 200 microliters of DMSO to each well. Measurements were made with a 570 nm SpectraMax i3 microplate reader device. The IC_{50} value was detected by a dose response inhibition panel graph at GraphPad Prism 6.0 software.

Preparation of 3D mono-culture and 3D co-culture, MTT cell viability assay

Each well of 96-well plates (VWR-734-2327, Nest) should be coated to prepare a non-adhesive surface. 3% agarose (BP160-100, Fisher Scientific) was prepared for the coating process. Huvec and Ishikawa cells were seeded in 96 well-plate coated with agarose for 3D mono-culture applications. For the mono-culture model, Huvec and Ishikawa cells were seeded at $1x10^4$ cells per well. For the coculture model, $5x10^3$: $5x10^3$ Huvec and Ishikawa cells were seeded per well. It was left to grow in an incubator with 5% CO_2 at 37 °C. Following the formation of spheroid forms, as we demonstrated in our previous study [24], 96-well microculture plates were treated with various concentrations (4-3-2-1-0.5 µM in DMSO) of FP-Oxa. Cells treated with % 0.1 TritonX-100 (Millipore, 108603) were used as the positive control group, and cells not treated with FP-Oxa formed the negative control group. After 24 hours of incubation, medium FP-Oxa mixtures were aspirated. The wells were washed with PBS so as not to damage the cells. 200 microliters of MTT (Vybrant® MTT Cell Proliferation Assay Kit) solution, diluted 1:20 in medium, was added to each well. MTT solutions were aspirated after 3 hours of incubation. Formazan salts were dissolved by adding 200 microliters of DMSO to each well. Measurements were made with a 570 nm SpectraMax i3 microplate reader device. The IC_{50} value was detected by a dose response inhibition panel graph at GraphPad Prism 6.0 software.

Demonstration of VEGF expressions in 3D co-cultures by immunofluorescent staining

The spheroids were treated for 24 hours with the determined IC_{50} values of the compound FP-Oxa. Spheroids not exposed to FP-Oxa were used as the control group. The spheroids were then transferred to an 8-well chamber (80841, Ibidi). For fixation, it was incubated for 20 minutes with 4% PFA (P6148, Sigma-Aldrich) diluted in 1X PBS (LM-S2041/500, Biosera) at room temperature. After aspirating 4% PFA, it was washed 3 times with 1X PBS for 5 minutes. Permeabilized with 0.1% Triton™ X-100 for 15 minutes. It was blocked with 2% BSA for 45 minutes at room temperature. The blocking solution was aspirated, washed 3 times with 1X PBS for 5 minutes. Spheroids were labeled with VEGF Monoclonal Antibody (JH121) (MA5-13182) at a 1:100 dilution in 0.1% BSA by incubation for 24 hours at +4°C. After the primary antibody was aspirated, it was washed 3 times with 1X PBS for 5 minutes. Secondary antibody diluted 1:2000 was added to the wells and incubated for 1 hour at room temperature. At the end of the incubation period, washing was done 3 times for 5 minutes with 1X PBS. The slide was covered with a coverslip solution containing DAPI (00-4959-52, Invitrogen). Three digital sections of equal thickness were taken and imaged from the spheroids using the Z Stack method via a Zeiss LSM 800 laser scanning confocal microscope. Measurements of VEGF densities of cells in all sections were analyzed and recorded with Zeiss Zen 2 Blue version. Expression levels were analyzed and compared semi-quantitatively.

Migration (Wound Healing) assay

As has been done in previous studies, Culture-Insert 2 Well in µ-Dish 35 mm (ibidi, Cat. No 80206) was used for a wound healing and migration experiment 3×10^5 cells were added in a 70 microliter medium each in two wells [25]. These were incubated at 37°C and 5 % CO_2 as usual. After appropriate cell attachment (24 hours), the Culture-Insert 2 Well was gently removed using sterile tweezers. IC_{50} value of the compound FP-Oxa was added to the experimental group cells in 2 mL doses. The migration rate in both experimental and control group cells was displayed at 0. and 24. hours. Wound closure rates were measured and recorded with the ImageJ software program.

Statistical analysis

MTT tests were performed in triplicate and data was represented as mean ± standard deviation (SD). Statistical significance was measured using analysis of variance (ANOVA one-way) and multiple comparisons test. Migration and immunofluorescence staining analyzes were evaluated with the Unpaired t test. Values were

processed using GraphPad Prism 5.0 software (San Diego, USA). $p < 0.05$ values were considered statistically significant.

RESULTS

Chemistry

In order to obtain the target compound (Fp-Oxa) in the study, starting from the phenylpiperazine compound (1), the ester compound (2) was obtained by reaction with ethyl bromoacetate, followed by nucleophilic addition reaction with hydrazine hydrate to give the hydrazide compound (3). Then, the target compound was synthesised by ring closure reaction of the hydrazide compound with CS_2 in the presence of KOH (Figure 1). FT-IR (υ_{max}, cm^{-1}): 3078.22 (ar-H), 2954.64 (aliphatic CH), 1633.61 (C=N). MALDI-TOF/MS: calculated: 276.104481; found: 278.078952 ($[M+2]^+$) (Figure S1, Figure S2).

Drug target identifcation (Druggability) and ADME analysis

SwissADME

Examining the ADME results range limits of the prediction algorithms, such as molecular weight, lipophilicity, polarity, saturation, number of rotatable bonds, H-bond acceptors and donors, AlogP, for drug applicability, it was seen that the synthesized compound was in the applicability zone and was therefore found to be safe (Table 2, Figure 2). All results can be accessible in Figure S3.

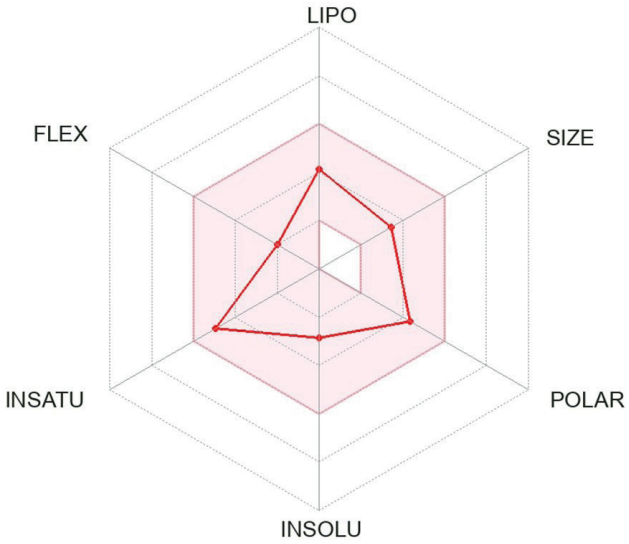

Figure 2. The colored zone is the suitable physicochemical space for oral bioavailability: LIPO (Lipophility): -0.7 < XLOGP3 < +5.0, SIZE : 150 g/mol < MW < 500 g/mol, POLAR (Polarity) : 20 $Å^2$ < TPSA < 130 $Å^2$, INSOLU (Insolubility) : -6.0 < Log S (ESOL) < 0, INSATU (Insaturation) : 0.25 < Fraction Csp3 < 1, FLEX (Flexibility) : 0 < Num. rotatable bonds < 9

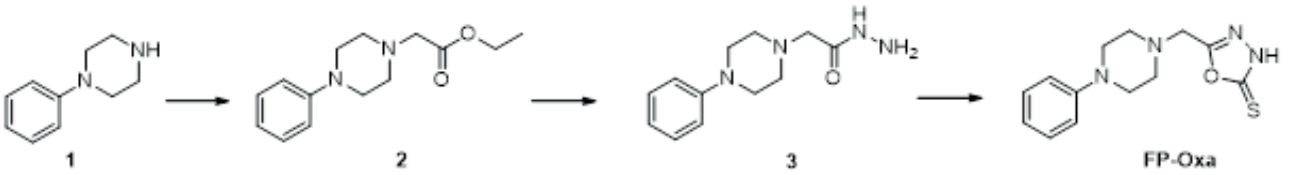

Figure 1. Synthetic schema for the target compound

Table 2. Limit values of drug applicability domains according to the SwissADME and the places of the target compound. The green color indicates that the compound obey the rules and is in domain. The red color indicates that the compound does not permeate into BBB and is not an inhibitor of CYP2C19

Molecular weight (g/mol)	TPSA (Å)	H-bond acceptors	H-bond donors	Lipophilicity (Log Po/w)	Water Solubility (Log S)	LogKp (skin permeation)	Druglikeness	Medicinal chemistry	Pharmacokinetics
276.36	84.20	4	0	1.59	-2.85	-6.78	Lipinski	PAINS	GI abs.[b]
							Ghose	Leadlikeness	BBB perm.[c]
							Weber	Syn. availability[a] (2.33)	P-gp subs.[d]
							Egan		CYP1A2 inhibitor
							Muegge		CYP2C19 inhibitor

[a] Synthetic availability. [b] Gastrointestinal absorption. [c] Blood Brain Barrier. [d] P-glycoprotein substrate.

Table 3. The calculated toxicity report by Pro Tox-II web-server of the compound

Classification	Target	Prediction	Probability
Organ Toxicity	Hepatotoxicity	Inactive	0.61
Toxicity End Points	Carcinogenicity	Active	0.60
Toxicity End Points	Immunotoxicity	Inactive	0.99
Toxicity End Points	Mutagenicity	Inactive	0.63
Tox21- Nuclear Receptor Signalling Pathways	Aryl Hydrocarbon Receptor	Inactive	0.76
Tox21- Nuclear Receptor Signalling Pathways	Androgen Receptor	Inactive	0.91
Tox21- Nuclear Receptor Signalling Pathways	Androgen Receptor Ligand Binding Domain	Inactive	0.95
Tox21- Nuclear Receptor Signalling Pathways	Aromatase	Inactive	0.80
Tox21- Nuclear Receptor Signalling Pathways	Estrogen Receptor Alpha	Inactive	0.83
Tox21- Nuclear Receptor Signalling Pathways	Estrogen Receptor Ligand Binding Domain	Inactive	0.95
Tox21- Nuclear Receptor Signalling Pathways	Peroxisome Proliferator Activated Receptor Gamma	Inactive	0.92
Tox21- Stress Response Pathways	Nuclear factor (erythroid-derived 2)-like 2/antioxidant responsive element	Inactive	0.85
Tox21- Stress Response Pathways	Heat Shock Factor Response Element	Inactive	0.85
Tox21- Stress Response Pathways	Mitochondrial Membrane Potential	Inactive	0.74
Tox21- Stress Response Pathways	Phosphoprotein Tumor Supressor p53	Inactive	0.88
Tox21- Stress Response Pathways	ATPase family AAA domain-containing protein 5	Inactive	0.92

Pro Tox-II

When the toxicity evaluation was examined, it was determined that the target compound showed toxicity within the limits determined for carcinogenicity and had a positive borderline toxicity value for hepatotoxicity and mutagenicity Table 3 and Figure S4 (Toxicity radar). Additionally, the compound is classified as toxicity class 4, where it is considered harmful if swallowed (300< LD50 ≤ 2000) (Figure 3).

SwissTargetPrediction

The target estimation of the chosen compounds was examined using the SwissTargetPrediction platform with the following investigations 15 of the outcomes depicted as a pie-chart (Figure S5). The compound was predicted as 6.7% Cytochrome P450 and 13.3% Family CG protein coupled-receptor.

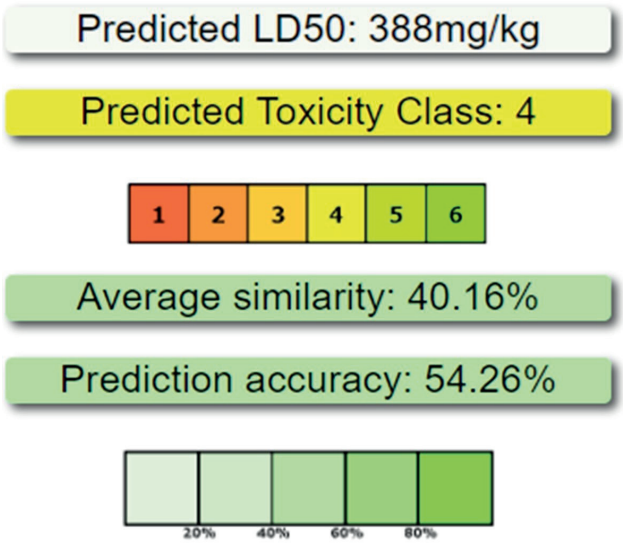

Figure 3. Toxicity classification of the compound

Boiled-egg

The BOILED-Egg profile which lets for intuitive consideration of passive gastrointestinal absorption (HIA) and brain penetration (BBB) in the function of the position of the molecules in the WLOGP-vs-TPSA referential was screened for the target compound. The white area is for the high probability of passive absorption by the gastrointestinal tract, while the yellow area is for the high probability of brain penetration. Also, the marks are colored in blue if predicted as actively effluxed by P-gp (PGP+) and in red if estimated as non-substrate of P-gp (PGP-). It was concluded that FP-Oxa was estimated well-absorbed but not accessing the brain, and it was also subject to active efflux (blue dot) (Figure S6).

Molecular Docking Studies

The 3D structure of VEGFR2 was downloaded from the protein database (PDB ID: 2OH4). SDF files of known VEGFR2 inhibitors and molecules including Ki20227, SKLB1002, CS-2660 (JNJ-38158471), Taxifolin (Dihydroquercetin) and Nintedanib (BIBF 1120) were prepared using DataWarrior. VGEFR2 inhibitors with IC_{50} values ranging from 12M to 40 nM were selected. After removing water and

small molecules from the construct, a grid box was created around the ATP binding pocket using AutoDockTools (Figure 4A). Automatic coupling of compounds was performed with PaDelADV. It was found that FP-Oxa showed higher binding affinity than the average of five known VEGFR2 inhibitors or three of the known VEFR2 inhibitors (SKLB1002, Taxifolin, Ki202227) (Figure 4B). FP-Oxa also docked well in the ATP binding pocket with a binding affinity of -7.2 kcal/mol, as observed in molecular docking studies (Figure 4C).

2D mono-culture and co-culture, MTT cell viability assay

2D cultured cells were treated with different doses of FP-Oxa (4-3-2-1-0.5 µM) for 24 hour. IC_{50} values determined in Ishikawa, Huvec and coculture cells at the end of the 24th hour are shown in Table 4. In all experimental models, a decrease in cell viability was observed in parallel with the increase in dose. In addition, analysis of cell viability percentages in doses was performed and calculated separately for each dose. Comparing the percentages of viability in Ishikawa and coculture cells, all drug dose groups, and untreated negative control cells,a highly significant difference was found with a value of ****: $p < 0.0001$ (Figure 5).

Table 4. IC_{50} values of 2D cells cultured with FP-Oxa for 24 hours

Cell Culture (2D)	IC_{50} (µM)	SEMa
Ishikawa	1.648	± 0.280
Huvec	1.591	± 0.254
Co-Culture	2.064	± 0.284

a: Standard Error Mean

3D mono-culture and co-culture, MTT cell viability assay

2D cultured cells were treated with different doses of FP-Oxa (4-3-2-1-0.5 µM) for 24 hour. IC_{50} values determined in Ishikawa, Huvec and coculture cells at the end of the 24th hour are shown in Table 5. Deviations were noted for the 1 µM dose group in 3D cultured Huvec cells and the 2 µM dose group

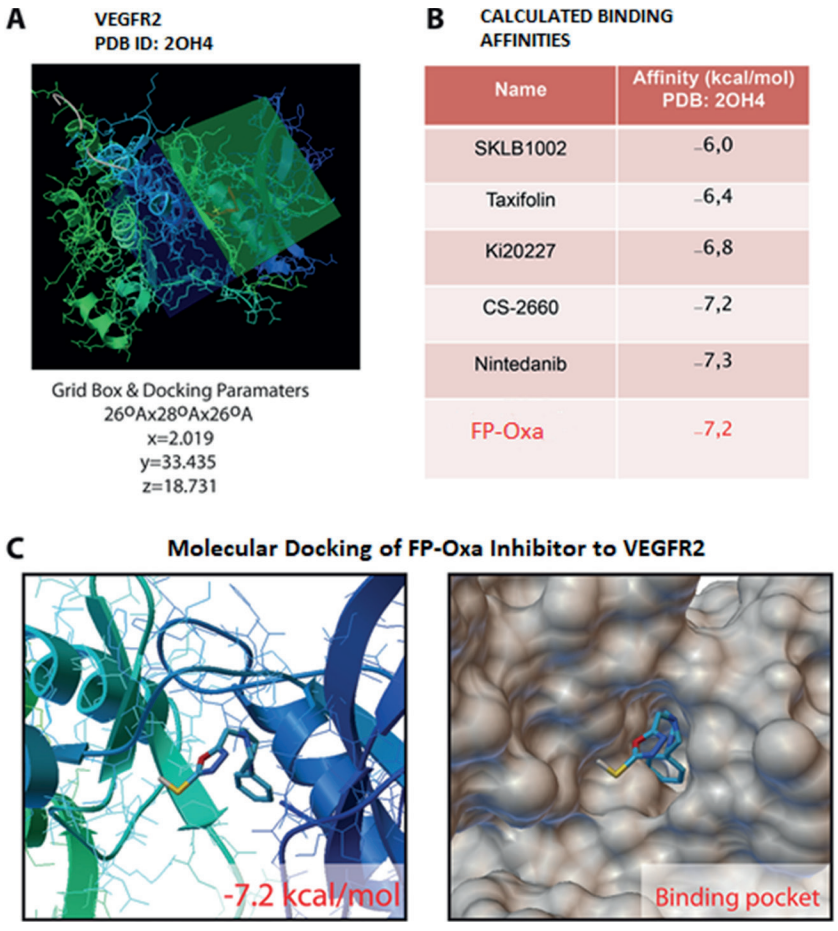

Figure 4. Molecular Docking of Compounds to VEGFR2 and Calculated Binding Affinities. A) VEGFR2 (PDB ID: 2OH4) 3D view and docking parameters. B) Calculated binding affinities via AutodockVina and PaDelAdv. C) Molecular Docking Pose of FP-Oxa Inhibitor to VEGFR2

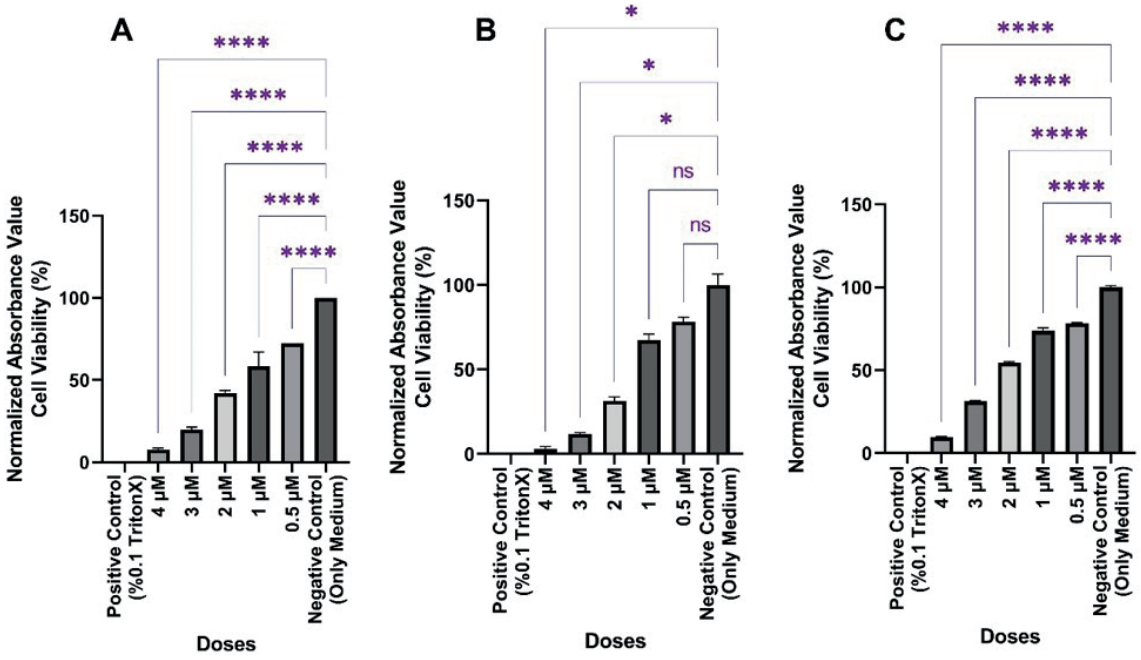

Figure 5. Dose-dependent percent viability plots of Ishikawa 2D culture (A), Huvec 2D culture (B), and Ishikawa, Huvec 2D Co-Culture (C) (****: Extremely significant, ***: Extremely significant, **: Very significant, *: Significant, ns: Not significant)

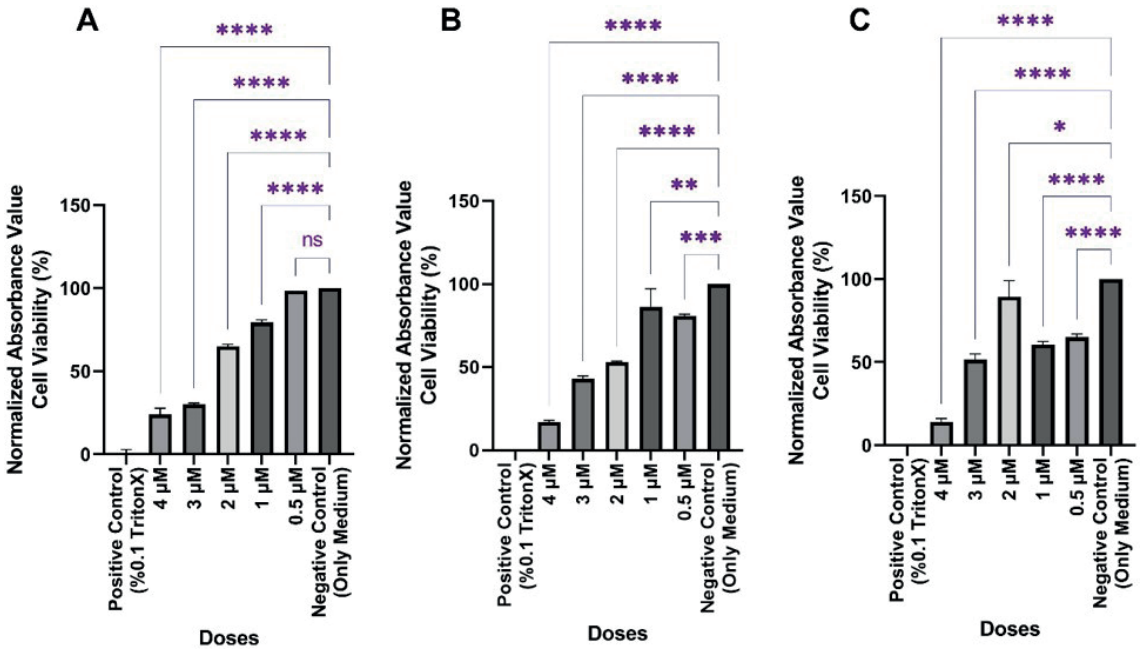

Figure 6. Dose-dependent percent viability plots of Ishikawa 3D culture (A), Huvec 3D culture (B), and Ishikawa, Huvec 3D Co-Culture (C) (****: Extremely significant, ***: Extremely significant, **: Very significant, *: Significant, ns: Not significant)

in 3D co-culture. Except for these dose groups, a decrease in cell viability was detected in all other dose groups due to dose increase (Figure 6).

VEGF expressions in 3D co-cultures

Images of the second sections corresponding to the middle part of the spheroids were added from the 3

Table 5. IC_{50} values of 3D cells cultured with FP-Oxa for 24 hours

Cell Culture (3D)	IC_{50} (µM)	SEM[a]
Ishikawa	2.384	± 0.437
Huvec	2.339	± 0.416
Co-Culture	2.755	± 0.793

a: Standard Error Mean

sections taken with the Z stack method (Figure 7A). Control 3D co-cultures and experimental group 3D co-cultures exposed to the compound FP-Oxa were compared for their integrated VEGF concentrations. It was observed that VEGF expression was decreased in the experimental group models with a significantly significant difference (**: p=0.0053) (Figure 7B).

Migration (Wound Healing) assay

2D cultured Ishikawa cells, Huvec cells, and co-cultures were treated with FP-Oxa for 24 h using predetermined IC_{50} doses. Cell groups not exposed to the FP-Oxa compound were used as controls. At the end of the 24th hour, all wound areas in the control group cells were closed (data not shown). There was no significant difference in the migration of Ishikawa cells when the proportion of wound areas closed at the end of 24 hours was compared with the control groups, while a very significant difference was observed in the Huvec cells (****: p< 0.0001) and Co-Culture groups (****: p< 0.0001) was recorded (Figure 8 A,B).

DISCUSSION

Drug-likeness contains structural, physicochemical, biochemical, pharmacokinetic, and toxicological parameters. On the other hand, ADME describes the absorption, distribution, metabolism, and excretion of a drug candidate compound. These two important processes specify the pharmacokinetic properties. Toxicity, efficacy, and inadequate pharmacokinetic properties are the reasons why compounds have not been able to be studied further or to market in drug discovery studies. Therefore, identifying these properties at the beginning of the study is an essential step for the ultimate clinical success of the compound. In our study, pharmacokinetic and toxicity evaluations were performed before the *in vitro* effects of the compound were demonstrated [26].

Bioavailability radar provides an at-a-glance understanding of the drug-likeness of the compound. The fact that the drug candidate compound is located within the borders of the colored region within the radar indicates that the compound is in the physicochemical area suitable for oral bioavailability. It was determined that the compound we used in our study and named FP-Oxa was within the appropriate limits for oral bioavailability (Figure 2). Toxicity assessment is very important in drug development before clinical trials are performed due to the fact that it is related to human health and the future of drug candidates. Due to the disadvantages of *in vitro* and *in vivo* toxicity studies, such as long duration, expensive and animal welfare, in silico toxicity calculations have been enhanced and become significant [27]. According to the results of the toxicity analysis, the compound was classified as toxicity class 4, which is considered harmful if ingested, with a prediction

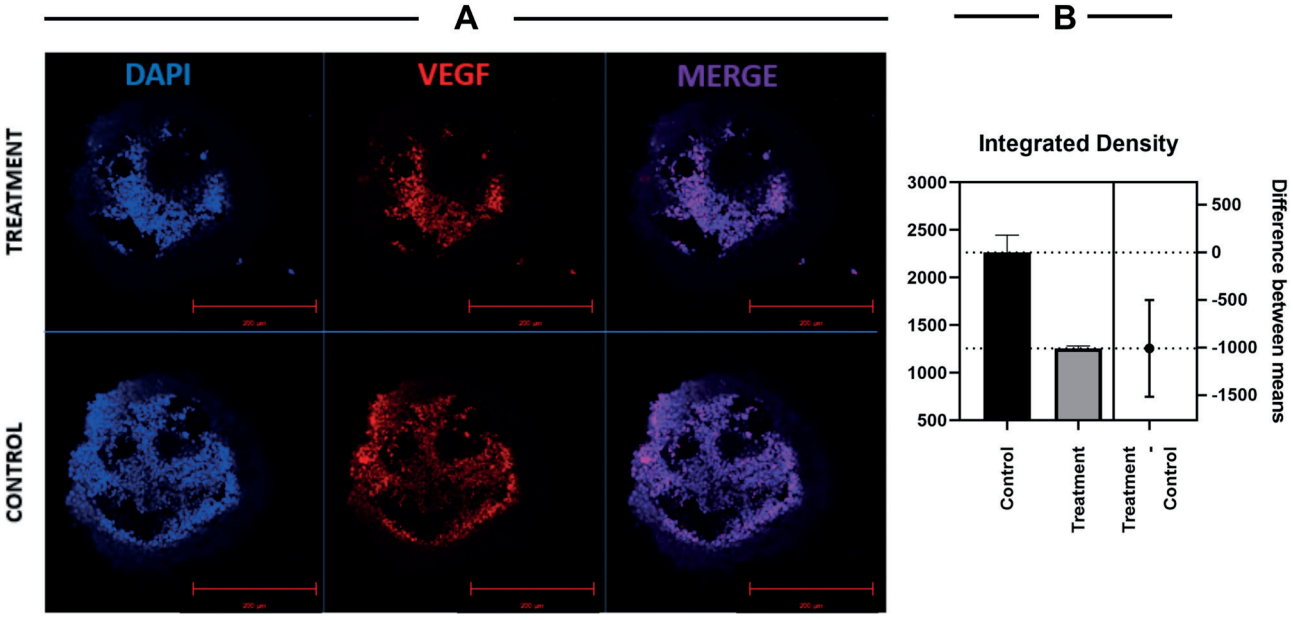

Figure 7. Confocal microscopic images of VEGF expressions of the 3D Co-Culture control and 3D Co-Culture treatment groups (A), VEGF expression rates integrated density from the control and treatment groups (B) (**: p=0,0053)

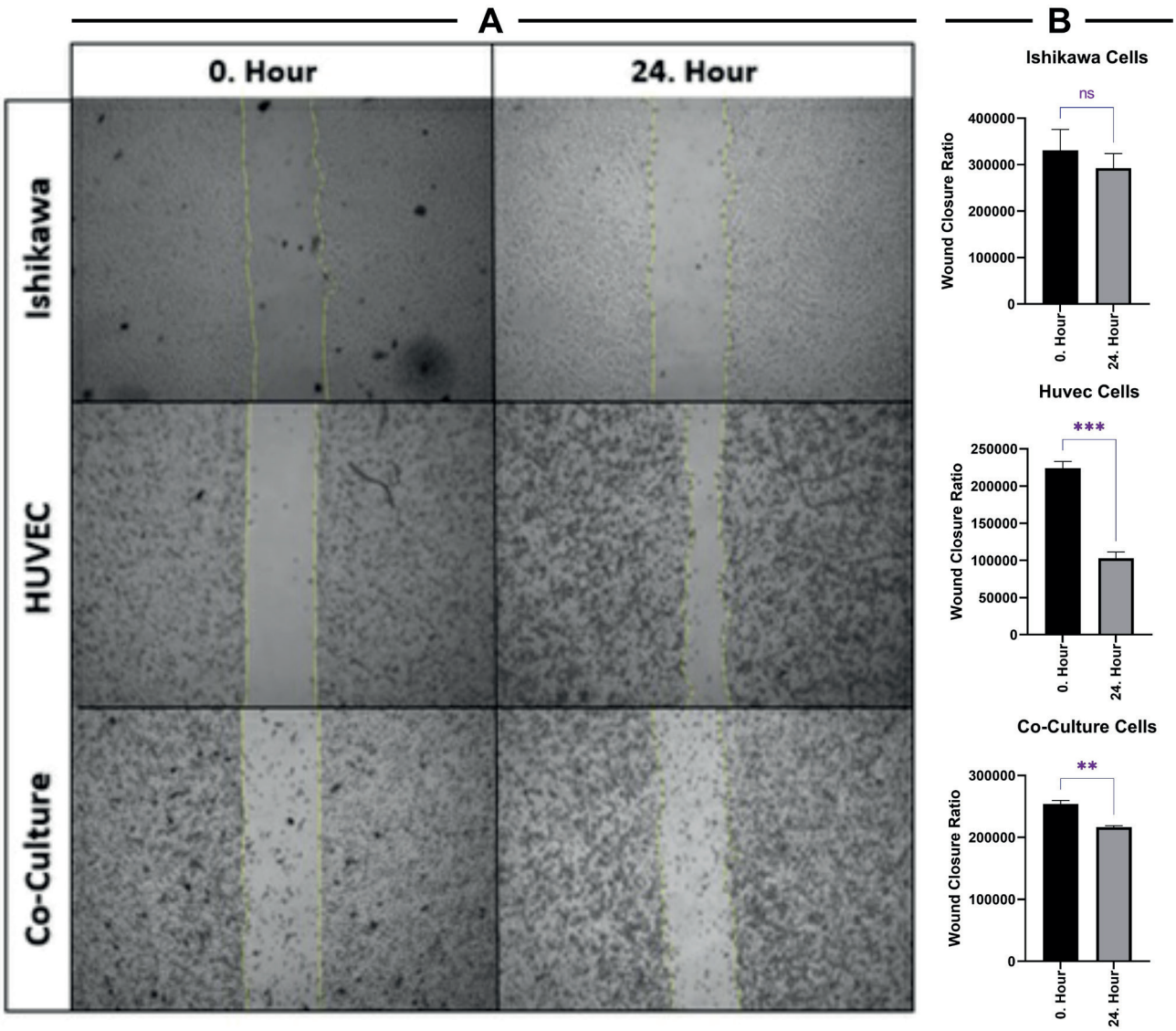

Figure 8. Wound healing areas in the treatment groups at 0. and 24. hours (A), Wound Closure rates at 0. and 24 Hours determined by field measurement (B)

accuracy rate of 54.26%. We think that the reason that may cause toxicity may be due to the presence of the -SH group in the structure of the compound (Figure 3). Additionally, it should not be overlooked that the toxicity results and class detected belong to rodents [28].

Molecular docking is a computational technique that predicts the binding affinity of ligands to receptor proteins [29]. By molecular docking calculations, the binding affinities of compounds to various receptors can be predicted, revealing their inhibition potential [30]. As a result of our molecular docking studies, it was determined that FP-Oxa has VEGFR2 inhibitor potential. When compared to the binding degrees of five compounds previously shown to be VEGFR2 inhibitors, it is promising that FP-Oxa has the best binding degree after Nintedanib (Figure 4). The affinity of the benzimidazole-urea inhibitor (PubChem CID 9935852) in the crystal structure (2OH4) of VEGFR2 was also determined. Our findings indicate a notable higher affinity (-10.6 kcal/mol) for VEGFR2, suggesting a more favorable fit into the inhibition pocket, particularly given the co-crystallization of this molecule with the target protein.

Cytochrome P450 (CYP) enzyme inhibition is the main mechanism in metabolism-based drug-drug interactions, and many chemotherapeutic drugs can cause drug interactions by inhibiting or inducing the CYP enzyme system [31]. CYPs have important roles in the metabolism of drugs that reduce cancer growth. Therefore, inhibitors of CYP

enzymes may potentially act as anticancer agents [32]. As a result of in silico prediction experiments, 6.7% binding of FP-Oxa to CYP can be considered as one of the reasons for switching to *in vitro* experiments (Figure S5).

The ability of anticancer drugs to pass through the blood-brain barrier is taken into account depending on the type of cancer. They are expected to exhibit this ability in tumors related to brain tissue [33]. However, it is not safe for the compound to be used in the treatment of endometrial cancer tumor to exhibit the ability to pass through the blood-brain barrier. In our study, the lack of ability of FP-Oxa to pass through the blood-brain barrier after boiled egg experiments is a promising result.

3D cultures are known to have more drug resistance than 2D cultures [34]. In our study, we found higher IC_{50} values in 3D culture models than in 2D culture models, which supports the literature (Table 4, Table 5).

Just like *in vivo* tumors, hypoxic areas deprived of nutrients and oxygen develop in the centers of tumor model spheroids [35]. This hypoxic state attracts VEGF-expressing endothelial cells towards cancer cells to provide adequate nutrients and oxygen, contributing to tumor progression and metastasis [36]. For these reasons, to ensure that VEGF was present in the medium, Ishikawa cells were co-cultured with VEGF-expressing Huvec cells as 3D spheroid models. Consistent with the molecular docking results, FP-Oxa was successful in significantly suppressing VEGF expression in 3D co-cultures compared with the control group (Figure 7).

As a result of the migration experiments we performed in conventional 2D cultures, FP-Oxa clearly suppressed the migration of Ishikawa cells cultured alone. FP-Oxa was not equally successful in Huvec cells cultured alone and in Huvec-Ishikawa co-cultures. At the end of the 24th hour, it was determined that a certain degree of closure had occurred in the wound areas in the Huvec and co-culture groups (Figure 8). However, it should not be overlooked that while the wound areas were completely closed at the end of the 24th hour in the control group cells, they were not completely closed in the Huvec and co-cultures. In the wound healing experiment, Ishikawa, Huvec and Co-culture cells were each exposed to their respective predetermined IC_{50} doses. This may therefore lead to the paradox that suppression of migration in Ishikawa cells may result from the death of the cells. However, the clear continuation of cell migration in the Huvec and Co-culture groups exposed to IC_{50} doses eliminates this contradiction. If we argue that the reason for migration suppression is due to cell death, we think that we should encounter the same situation in Huvec and Co-culture groups.

This study shows how an oxadiazole derivative, which we call FP-Oxa, affects viability, migration, and angiogenesis in models co-cultured with Ishikawa cells and Huvec cells. In this respect, encouraging research on the effect of FP-Oxa on other types of cancer may contribute to the field. However, the results regarding VEGF expression were revealed semi-quantitatively. This situation can be considered as a limitation of the study. In future studies, it will be important to determine the amount of VEGF expression quantitatively at the mRNA level, to reveal the molecular pathway through which the cell death mechanism continues, and to investigate the biological activities of FP-Oxa in different types of cancer.

Author contribution

Study conception and design: MB, AM, and FK; data collection: MB, BE, and MK; analysis and interpretation of results: MB, AM, MK and IK; draft manuscript preparation: MB, FK, BE and IK. All authors reviewed the results and approved the final version of the manuscript.

Ethical approval

Since the study is a cell culture study performed on commercially purchased cell lines, it is not subject to ethical approval.

Funding

This study was supported by Istanbul Medipol University Scientific Research Projects commission with project number 2020/07.

Conflict of interest

The authors declare that there is no conflict of interest.

REFERENCES

[1] Moore K, Brewer MAJASoCOEB. Endometrial cancer: is this a new disease? 2017;37:435-442.

[2] Berek JS, Hacker NFJ. Practical gynecologic oncology. 2005.

[3] Ueda Y, Miyake T, Egawa-Takata T, et al. Second-line chemotherapy for advanced or recurrent endometrial carcinoma previously treated with paclitaxel and carboplatin, with or without epirubicin. 2011;67:829-835.

[4] Makker V, Green AK, Wenham RM, et al. New therapies for advanced, recurrent, and metastatic endometrial cancers. 2017;4(1):1-12.

[5] Sivridis E, Giatromanolaki A, Koukourakis MIJTJoPAJotPSoGB, Ireland. The vascular network of tumours—what is it not for? 2003;201(2):173-180.

[6] Gospodarowicz D, Abraham J, Schilling JJPotNAoS. Isolation and characterization of a vascular endothelial cell mitogen produced by pituitary-derived folliculo stellate cells. 1989;86(19):7311-7315.

[7] Oplawski M, Dziobek K, Zmarzły N, et al. Expression profile of VEGF-C, VEGF-D, and VEGFR-3 in different grades of endometrial cancer. 2019;20(12):1004-1010.

[8] Kudo M, Finn RS, Qin S, et al. Lenvatinib versus sorafenib in first-line treatment of patients with unresectable hepatocellular carcinoma: a randomised phase 3 non-inferiority trial. 2018;391(10126):1163-1173.

[9] Awasthi N, Hinz S, Brekken RA, Schwarz MA, Schwarz REJCl. Nintedanib, a triple angiokinase inhibitor, enhances cytotoxic therapy response in pancreatic cancer. 2015;358(1):59-66.

[10] Allen E, Walters IB, Hanahan DJCCR. Brivanib, a dual FGF/VEGF inhibitor, is active both first and second line against mouse pancreatic neuroendocrine tumors developing adaptive/evasive resistance to VEGF inhibition. 2011;17(16):5299-5310.

[11] Aparicio S, Sawant S, Lara N, Barnstable C, Tombran-Tink JJB, communications br. Expression of angiogenesis factors in human umbilical vein endothelial cells and their regulation by PEDF. 2005;326(2):387-394.

[12] Bahcecioglu G, Basara G, Ellis BW, Ren X, Zorlutuna PJAb. Breast cancer models: Engineering the tumor microenvironment. 2020;106:1-21.

[13] Friedrich J, Seidel C, Ebner R, Kunz-Schughart LAJNp. Spheroid-based drug screen: considerations and practical approach. 2009;4(3):309-324.

[14] Zschenker O, Streichert T, Hehlgans S, Cordes NJPo. Genome-wide gene expression analysis in cancer cells reveals 3D growth to affect ECM and processes associated with cell adhesion but not DNA repair. 2012;7(4):e34279.

[15] Andreani A, Granaiola M, Leoni A, Locatelli A, Morigi R, Rambaldi MJEjomc. Synthesis and antitubercular activity of imidazo [2, 1-b] thiazoles. 2001;36(9):743-746.

[16] Banik BK, Sahoo BM, Kumar BVVR, et al. Green synthetic approach: An efficient eco-friendly tool for synthesis of biologically active oxadiazole derivatives. 2021;26(4):1163.

[17] Shahzad SA, Yar M, Bajda M, et al. Synthesis and biological evaluation of novel oxadiazole derivatives: A new class of thymidine phosphorylase inhibitors as potential anti-tumor agents. 2014;22(3):1008-1015.

[18] Mermer A, Faiz O, Demirbas A, Demirbas N, Alagumuthu M, Arumugam S. Piperazine-azole-fluoroquinolone hybrids: Conventional and microwave irradiated synthesis, biological activity screening and molecular docking studies. Bioorg Chem. 2019;85:308-318.

[19] Bakchi B, Krishna AD, Sreecharan E, et al. An overview on applications of SwissADME web tool in the design and development of anticancer, antitubercular and antimicrobial agents: A medicinal chemist's perspective. 2022;1259:132712.

[20] Banerjee P, Eckert AO, Schrey AK, Preissner RJNar. ProTox-II: a webserver for the prediction of toxicity of chemicals. 2018;46(W1):W257-W263.

[21] Gfeller D, Grosdidier A, Wirth M, Daina A, Michielin O, Zoete VJNar. SwissTargetPrediction: a web server for target prediction of bioactive small molecules. 2014;42(W1):W32-W38.

[22] Daina A, Zoete VJC. A boiled-egg to predict gastrointestinal absorption and brain penetration of small molecules. 2016;11(11):1117-1121.

[23] Kocabas F, Xie L, Xie J, et al. Hypoxic metabolism in human hematopoietic stem cells. Cell Biosci. 2015;5(1):39.

[24] Kalender M, Bulbul MV, Kolbasi B, Keskin IJAPJoCPA. In 2D and 3D Cell Culture Models, Effects of Endothelial Cells on E-cadherin/β-catenin Expression Levels and Spheroid Sizes in Ishikawa Cells. 2022;23(1):39.

[25] Bulbul MV, Karabulut S, Kalender M, Keskin I. Effects of Gallic Acid on Endometrial Cancer Cells in Two and Three Dimensional Cell Culture Models. Asian Pac J Cancer Prev. 2021;22(6):1745-1751.

[26] Cruciani G, Pastor M, Guba WJEJoPS. VolSurf: a new tool for the pharmacokinetic optimization of lead compounds. 2000;11:S29-S39.

[27] Zhang L, Zhang H, Ai H, et al. Applications of machine learning methods in drug toxicity prediction. 2018;18(12):987-997.

[28] Drwal MN, Banerjee P, Dunkel M, Wettig MR, Preissner RJNar. ProTox: a web server for the in silico prediction of rodent oral toxicity. 2014;42(W1):W53-W58.

[29] Agu P, Afiukwa C, Orji O, et al. Molecular docking as a tool for the discovery of molecular targets of nutraceuticals in diseases management. 2023;13(1):13398.

[30] Pantsar T, Poso AJM. Binding affinity via docking: fact and fiction. 2018;23(8):1899.

[31] Manikandan P, Nagini SJCdt. Cytochrome P450 structure, function and clinical significance: a review. 2018;19(1):38-54.

[32] Wahlang B, Falkner KC, Cave MC, Prough RAJAiP. Role of cytochrome P450 monooxygenase in carcinogen and chemotherapeutic drug metabolism. 2015;74:1-33.

[33] Angeli E, Nguyen TT, Janin A, Bousquet GJIjoms. How to make anticancer drugs cross the blood–brain barrier to treat brain metastases. 2019;21(1):22.

[34] Shehzad A, Ravinayagam V, AlRumaih H, et al. Application of three-dimensional (3D) tumor cell culture systems and mechanism of drug resistance. 2019;25(34):3599-3607.

[35] Ohnishi K, Tani T, Bando S-I, et al. Plastic induction of CD133AC133-positive cells in the microenvironment of glioblastoma spheroids. 2014;45(2):581-586.

[36] Wilson WR, Hay MPJNRC. Targeting hypoxia in cancer therapy. 2011;11(6):393-410.

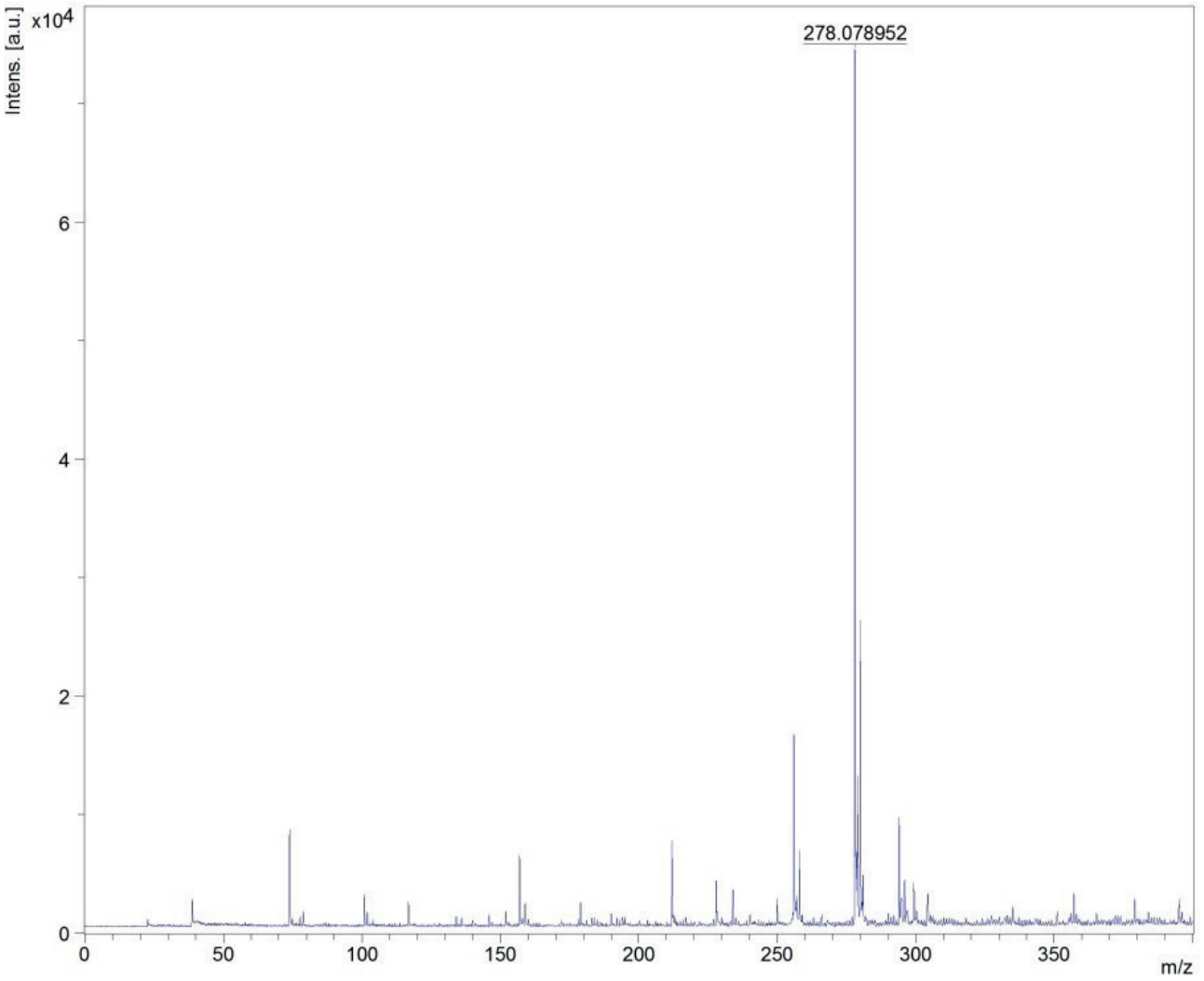

Figure S1. Title

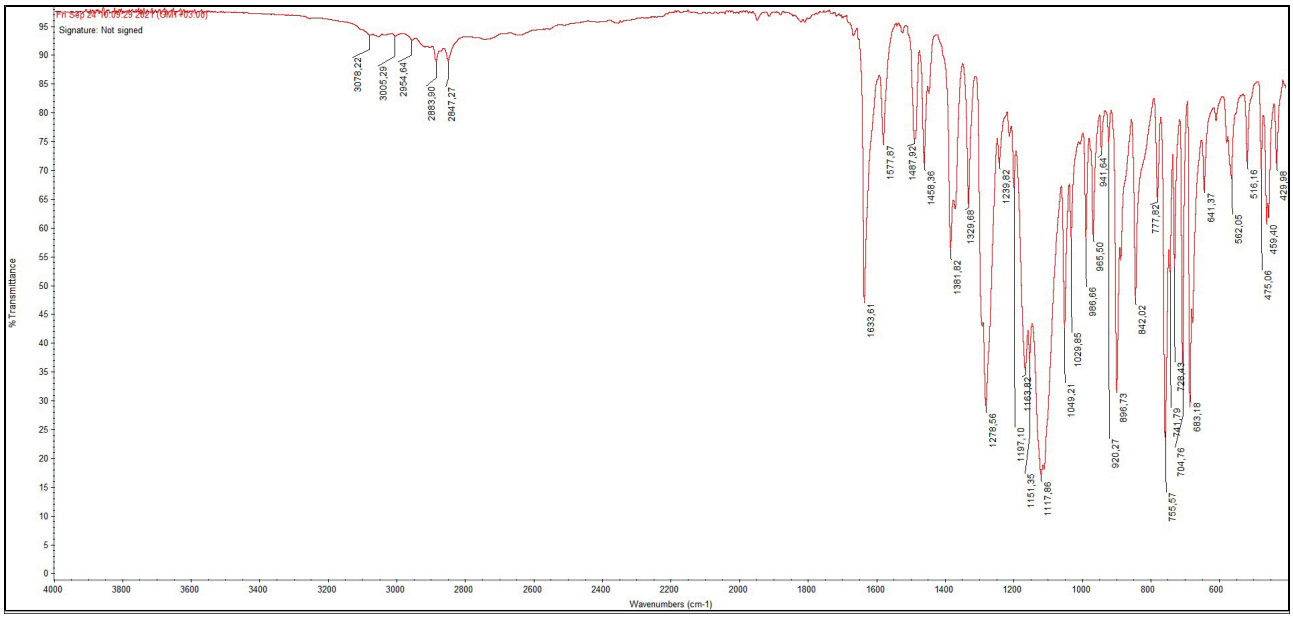

Figure S2. Title

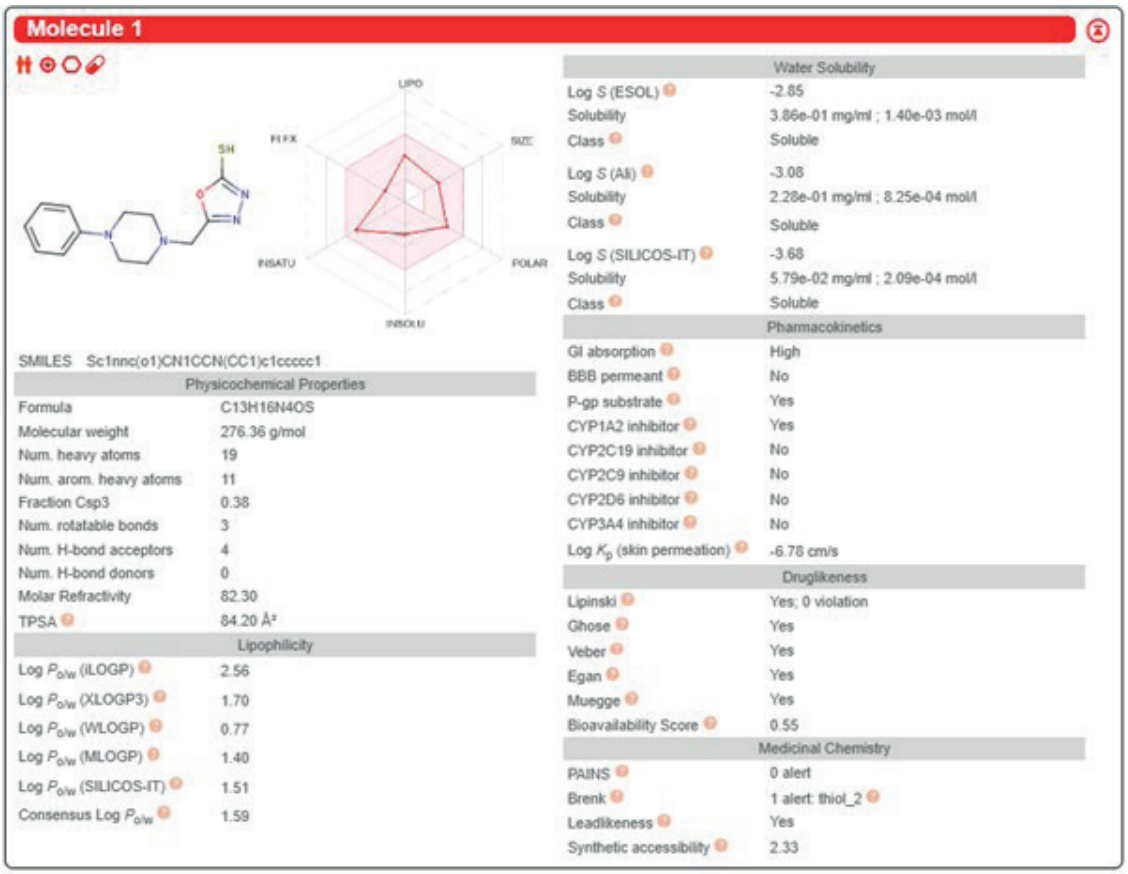

Figure S3. Title

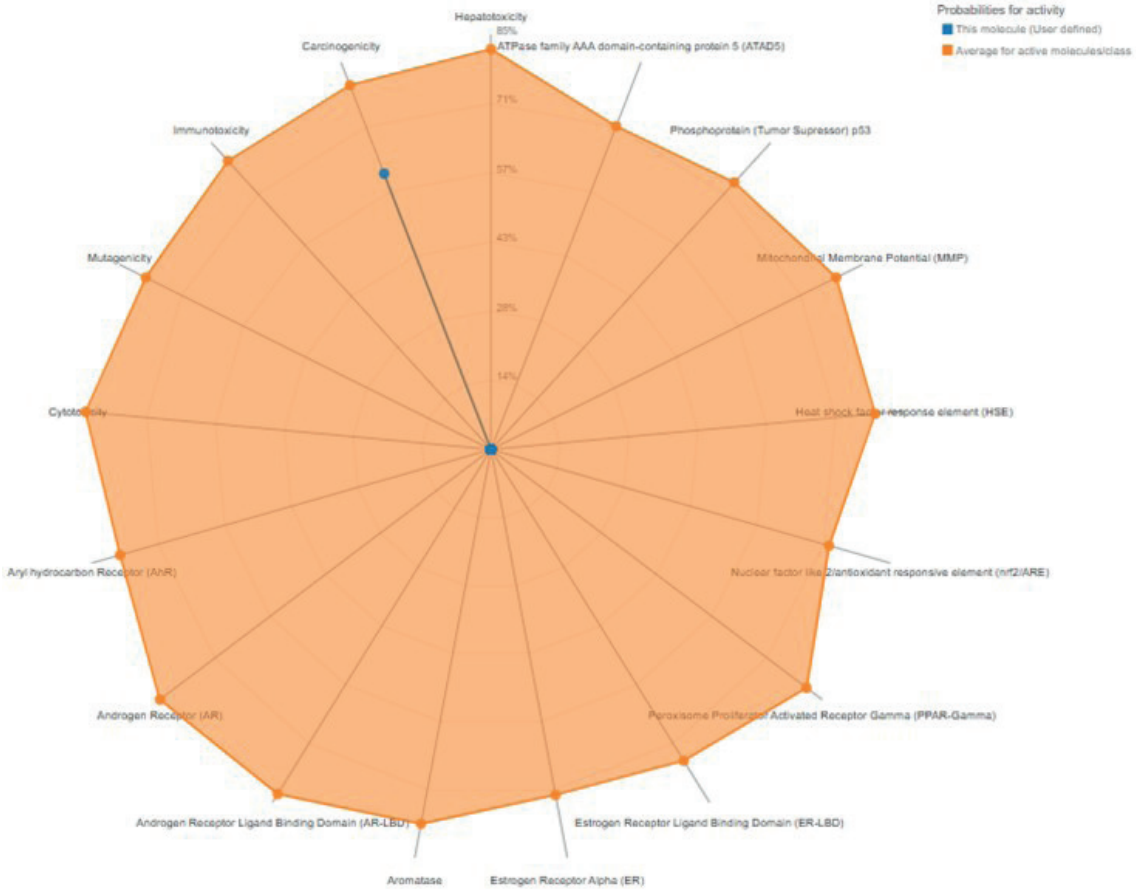

Figure S4. Title

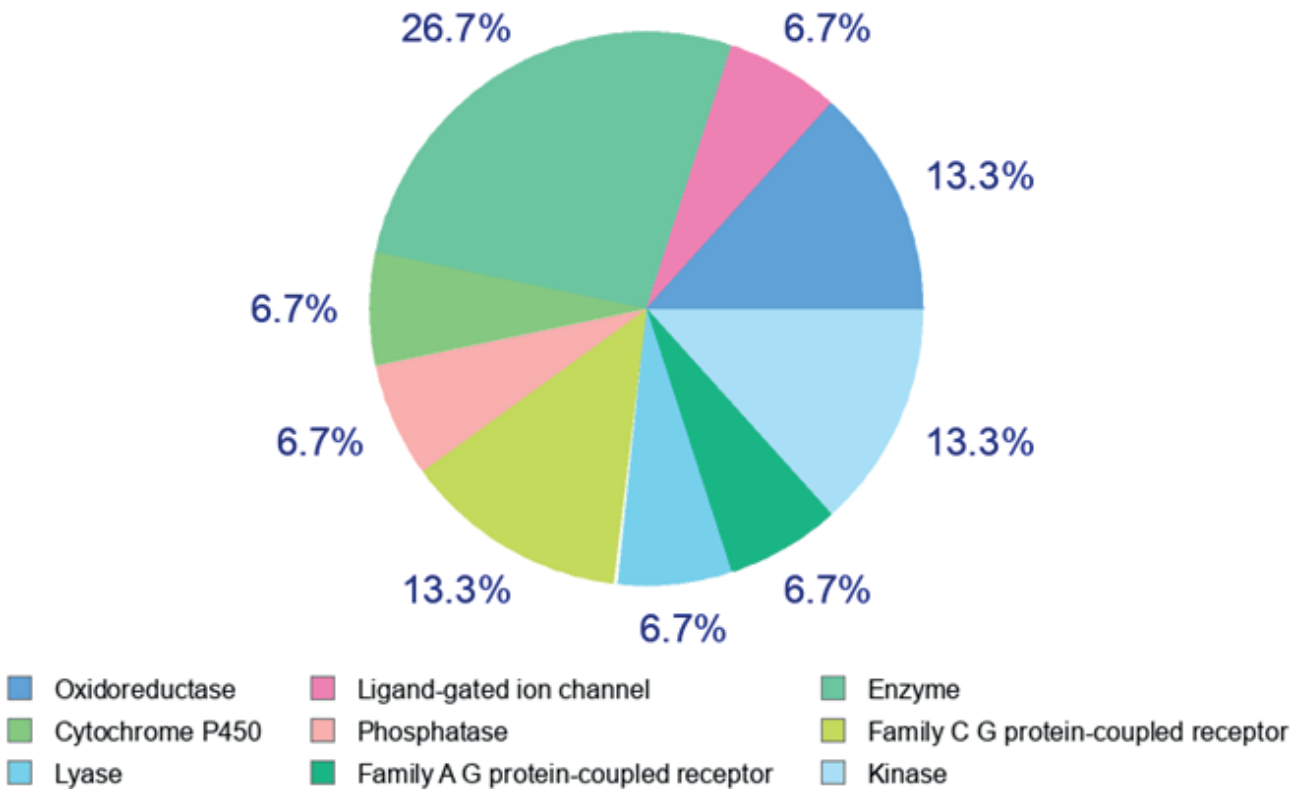

Figure S5. Title

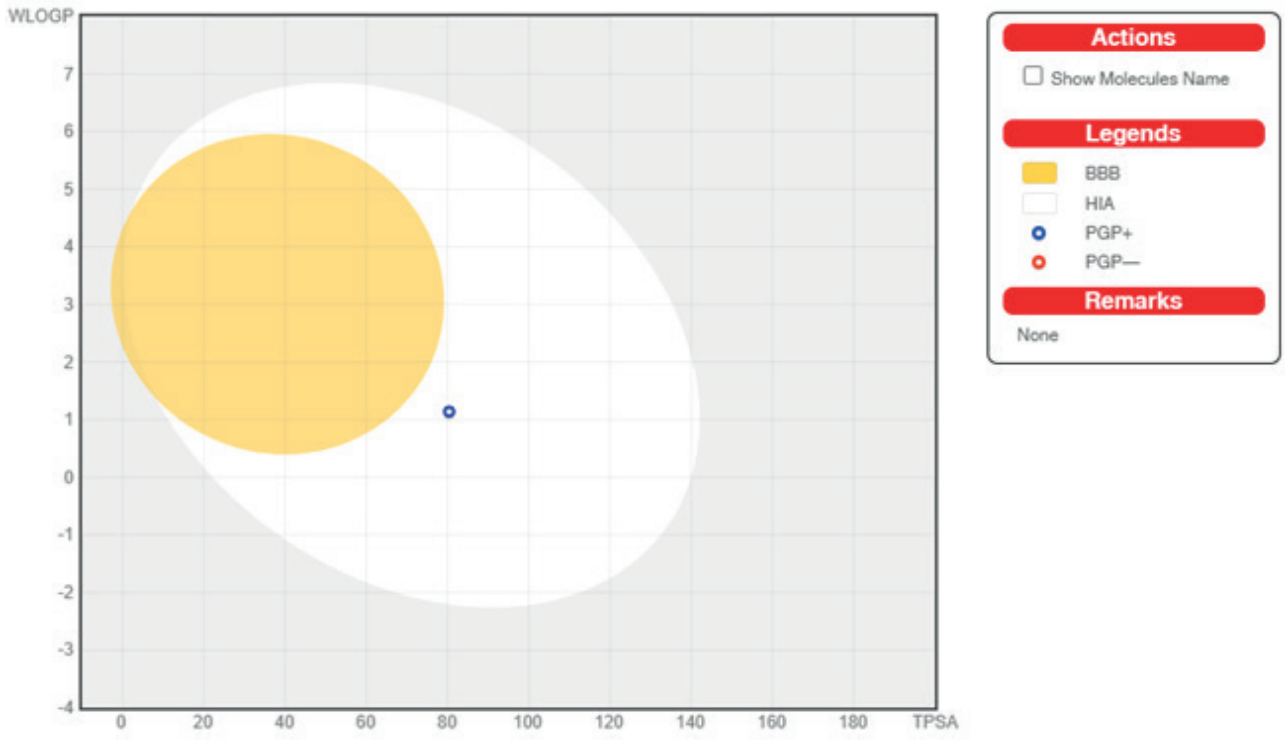

Figure S6. Title